Regional Cerebral Blood Flow Correlations of Somatosensory Areas 3a, 3b, 1, and 2 in Humans During Rest: A PET and Cytoarchitectural Study

Jeremy P. Young,[1,2]* **Stefan Geyer,**[3] **Christian Grefkes,**[3] **Katrin Amunts,**[4] **Patricia Morosan,**[3] **Karl Zilles,**[3,4] **and Per E. Roland**[1]

[1]*Division of Human Brain Research, Department of Neuroscience, Karolinska Institute, Stockholm, Sweden*
[2]*Department of Physiology, University of Sydney, Sydney, Australia*
[3]*Department of Neuroanatomy and C & O Vogt Brain Research Institute, Heinrich Heine University, Duesseldorf, Germany*
[4]*Institute for Medicine, Research Centre, Juelich, Germany*

◆ ═══════════════════════════════════ ◆

Abstract: The concept of functional connectivity relies on the assumption that cortical areas that are directly anatomically connected will show correlations in regional blood flow (rCBF) or regional metabolism. We studied correlations of rCBF of cytoarchitectural areas 3a, 3b, 1, and 2 in the brains of 37 subjects scanned with PET during a rest condition. The cytoarchitectural areas, delineated from 10 postmortem brains with statistical methods, were transformed into the same standard anatomical format as the resting PET images. In areas 3a, 3b, and 1, somatotopically corresponding regions were intercorrelated. Area 2 was correlated with the dorsal pre-motor area. These results were in accordance with the somatosensory connectivity in macaque monkeys. In contrast, we also found correlations between areas 3b and 1 with area 4a, and SMA, and among the left and right hand sector of areas 3a, 3b, and 1. Furthermore, there were no correlations between areas 3b, 1, and 2 with SII or other areas in the parietal operculum, nor of other areas known to be directly connected with areas 3a, 3b, 1, and 2 in macaques. This indicates that rCBF correlations between cortical areas during the rest state only partly reflect their connectivity and that this approach lacks sensitivity and is prone to reveal spurious or indirect connectivity. *Hum. Brain Mapping 19:183–196, 2003.* © **2003 Wiley-Liss, Inc.**

Key words: human; somatosensory; rCBF; rest state; correlations; anatomical; functional; connectivity; PET

◆ ═══════════════════════════════════ ◆

INTRODUCTION

Horwitz and colleagues [1984] introduced studies in which the correlations of regional cerebral blood flow (rCBF), or regional cerebral metabolism (rCMR), among brain regions were examined to reveal their functional connectivity. Later, studying correlations of the blood-oxygenation-level-dependent (BOLD) sig-

nals among brain regions were introduced. In these earlier studies, the authors measured these variables in the brain whilst the subject performs a predefined behavioral task, or function [Friston, 1994; Horwitz et al., 1984; Horwitz, 1994]. This was referred to as "functional connectivity."

A more recent alternative approach has been to examine correlations between brain regions of rCBF, rCMR, or BOLD signals whilst the subject performs no task in particular, such as during a rest state condition. It has been shown that the low-frequency temporal fluctuations in BOLD signals during rest can be attributed to brain activity rather than to extra-cerebral sources of noise [Cordes et al., 2001]. Correlations of the BOLD signal among brain regions during rest may also closely resemble the correlations during a task activation state [Cordes et al., 2001]. The temporal fluctuations of the BOLD signal in the primary motor cortex at rest was found to be correlated with those in several other brain regions associated with motor function [Biswal et al., 1995]. Xiong et al. [1999] noted that resting state correlations provide more information about brain regions interacting with the primary motor cortex than an analysis of a task-induced activation. Assuming that the observed correlations represented anatomical connections between brain regions, Xiong et al. [1999] concluded that the connectivity inferred from the correlations with the motor region of interest ROI was similar to that of established primate connectivity.

Linking correlations in rCBF, rCMR, or BOLD at rest with anatomical connectivity is an attractive concept, since it is presently not possible to directly trace in detail the anatomical connections either between different cortical regions in the intact human brain or in post-mortem material, except for short-range cortical connections [Burkhalter et al., 1993; Galuske et al., 2000]. However, diffusion tensor imaging is emerging as a promising technique for tracing white-matter tracts in vivo. Furthermore, the connectivity of the human brain cannot be inferred from macaque studies, unless the areas under study are homologous. The concept of linking correlations with connectivity, however, relies on a number of assumptions.

Firstly, it is assumed that spontaneous neural activity exists in humans [Llinas, 1988; Steriade et al., 1993], that is, action potentials that are simply the consequence of being awake, but not related to any particular thinking, task, or behavior. Secondly, that spontaneous neural activity occurs while a human subject is not performing any task in particular, as is the case during the classical rest state condition in neuroimag-

ing studies [Larsen et al., 1978]. Thirdly, that if two brain regions, A and B, are directly connected anatomically by mutual excitatory connections, then the neural activity in region A will invoke neural activity in region B, and vice versa. Therefore, the neural activity of A and B would correlate [Horwitz, 1994]. Since neural activity and regional cerebral blood flow (rCBF) are tightly coupled [Olesen et al., 1971], brain regions, A and B, should also correlate their rCBF. The rCBF can be measured with positron emission tomography (PET). Therefore, based on these assumptions, neural activity in the human can be measured indirectly via rCBF at rest, and correlations among brain regions can reveal patterns of connectivity. There are limitations of linking correlations with connectivity. Two main limitations include (1) the inability to determine the direction of connectivity, and (2), when three or more regions correlate, it is not possible to determine whether the correlations are due to direct or indirect connectivity.

A bias that affects all previous correlation studies of neuroimaging data concerns the selection of the regions among which the correlations are to be calculated. Defining a test region usually requires the subject to perform a task to functionally activate a particular brain region of interest. This method relies on the assumption that the activated region is functionally homogeneous. Furthermore, the activated region is used to delineate the anatomical region of brain defined as the test region. Thus, the investigator further assumes that the functionally activated area is also anatomically homogeneous. Another bias concerns the anatomical localization of correlated brain regions. The currently established and generally accepted method for anatomical localization is to overlay the resultant functional image with the high resolution MRI. However, it is not possible for the investigator to identify any cortical area from MRI scans [Roland and Zilles, 1996a, 1998]. Therefore, it is not possible to ensure that the underlying anatomy of a functional image is homogeneous.

In the present study, we used a new unbiased approach so that the selection of the test region from probability maps of cortical areas delineated by cytoarchitectonic mapping in post-mortem human brains is independent from the PET data subjected to correlation analysis. Somatosensory areas 3a, 3b, 1, and 2 were cytoarchitecturally delineated. First, we calculated the correlation matrix of all cytoarchitecturally delineated somatosensory and motor areas, and then we calculated the correlations in rCBF between the cytoarchitectural areas 3a, 3b, 1, and 2 with the rest of

the brain. By investigating the human somatosensory areas, we could directly relate correlation patterns with established macaque connectivity patterns since the somatosensory areas 3a, 3b, 1, and 2 of both species are homologous [Zilles et al., 1995].

Using rest state rCBF in areas 3a, 3b, 1, and 2, the aim of this study was to investigate correlations in rCBF (1) between these areas, ipsilaterally and contralaterally, (2) with surrounding motor areas, and (3) to test for additional correlations with other brain regions. We hypothesized that if the pattern of rest state correlations of somatosensory areas in the human brain were similar to the pattern of the known anatomical connectivity of homologous somatosensory areas 3a, 3b, 1, and 2 in the macaque, then this supports spontaneous neural activity as the dominant drive of neural activity in the human brain during rest, and, thus, the inference of connectivity schemes in the human may be possible.

The correlations among the human somatosensory areas 3a, 3b, 1, and 2 in many respects fit with established connectivity schemes from the macaque monkey. However, correlations were also found that did not correspond to the connectivity of macaque areas and, conversely, areas that are interconnected in the macaque failed to correlate their rCBF.

SUBJECTS AND METHODS

Condition

Subjects were scanned whilst in a rest state [Roland and Larsen, 1976]. The subjects had their eyes closed and covered with a cotton wool pad and mask. They were instructed to relax, and not to think of anything in particular during each resting scan. Sham injections were used before the actual PET measurement to habituate the subjects to the scanning conditions. On completion of the scan, the subjects were questioned as to what they experienced during the scan. Subjects were specifically questioned on whether they heard, felt, or saw anything that disturbed them during the scanning period. Subjects were observed for movements during the scan. If the subject moved, reported being disturbed, or preoccupied with imagery, the scan was excluded and repeated. The resting state PET scan was repeated three times on each subject in a randomized schedule with other tasks in the same experiment. No resting state conditions were the very first scan of an experiment and no voluntary movements were observed during the scans included in this study.

Subjects

The Ethics and Radiation Safety Committees of the Karolinska Institute and Hospital approved the studies and all subjects gave informed consent. Thirty-eight healthy male volunteers (24 to 40 years, mean 29 years) participated in this PET study. They had no history of neurological diseases. All subjects were right-handed as determined by the Edinburgh inventory [Oldfield, 1971]. The data presented here have not been published before.

Scanning

The methods for 3-D–PET measurements of the regional cerebral blood flow (rCBF) have been described in detail earlier [Hadjikhani and Roland, 1998]. Briefly, individually molded thermoplastic helmets [Bergström et al., 1981] were used for stereotaxic alignment of the subject's head during both MRI and PET scans. Prior to the PET scanning sessions, a T-1 weighted high-resolution anatomical magnetic resonance (MR) scan was acquired (3-D–SPGR, TE = 5 msec, TR = 21 msec, flip angle = 50 degrees, FOV = 256 mm, matrix 124 slices) on a 1.5 Tesla GE scanner (Signa Horizon Echospeed, General Electric Medical Systems, Milwaukee, WI). The rCBF was measured using a CTI-Siemens ECAT EXACT HR PET scanner (FOV = 150 mm, FWHM = 3.8 mm) in 3-D mode. A bolus injection of ^{15}O butanol was used as the tracer (approximately 14 mCi per scan) for each scan. The subjects rested in the supine position with their head positioned by the helmet in the PET scanner. The tracer was administered through the catheter placed in the right brachial vein. The arterial tracer concentration was continuously and automatically monitored via a left radial artery catheter. The PET images were reconstructed with either a Ramp or 4 mm Hanning filter. An autoradiographic method [Meyer, 1989] was used to calculate the rCBF during the 50-sec period after the tracer reached the brain. The PET scans in each subject were spatially aligned to the first PET scan, and subsequently aligned to the anatomical MRI, by the AIR software [Woods et al., 1992].

Transformation into standard anatomical format

Standard dilation, erosion, and manual editing techniques were used to remove non-brain matter from the MRI of each of the 38 subjects. The MRI of each subject was aligned to the Standard Brain of the Human Brain Atlas (HBA) [Roland et al., 1994] using a

two-step procedure incorporating an extended principle axes transformation (PAT) [Woods et al., 1992] and the automated full-multigrid method (FMG) [Schormann and Zilles, 1998]. Each MRI alignment produced a set of parameters that were subsequently applied to the three resting state PET images of the same subject.

A total of 114 resting state PET images, transformed into standard space, were used in this analysis. The PET images were smoothed with a 3-D isotropic Gaussian kernel with a full width at half maximum of 6 mm.

Cytoarchitectural areas

The following procedures were used to define the volumes of interest (VOI) in this study. Somatosensory areas 3a, 3b, 1 [Geyer et al., 1999] and 2 [Grefkes et al., 2001], motor areas 4a and 4p [Geyer et al., 1996], visual areas 17 and 18 [Amunts et al., 2000], Broca's areas 44 and 45 [Amunts et al., 1999], and auditory areas Te 1.0, 1.1, and 1.2 [Morosan et al., 2001] were delineated in 10 postmortem brains by an observer-independent cytoarchitectonic technique, described in detail by Schleicher et al. [1999]. Briefly, histological serial sections (20 μm thick) of 10 postmortem adult human brains were silver stained for cell bodies. The histological sections were matched with a previously acquired MR image of the same brain prior to fixation and sectioning, to account for histological procedural artifacts. A quantitative observer-independent method based on the grey level index (GLI) was used to measure cortical laminar densities of neurons and to determine borders between cytoarchitectonic areas [Schleicher et al., 1999]. Each delineated cytoarchitectural area was reconstructed as a 3-dimensional digital image and aligned with a PAT and FMG procedure to the HBA standard brain. A population map [Roland and Zilles, 1998] was generated by superimposing corresponding cytoarchitectural areas of each postmortem brain in standard anatomical (HBA) 3-D space. From the population map, each cytoarchitectural area was defined by voxels having a higher probability of belonging to this area than to any other area. This produced the cytoarchitectural probability map. The anatomically standardized probability map was checked against the anatomically standardized MR images, to verify that the bottom of the central sulcus corresponded to the border between area 3a and area 4p.

Somatotopically organized areas (areas 3a, 3b, and 1) were further subdivided into hand, face, and lower body regions. The extent of the hand region was determined (Talairach co-ordinates z = 34 to 58) from
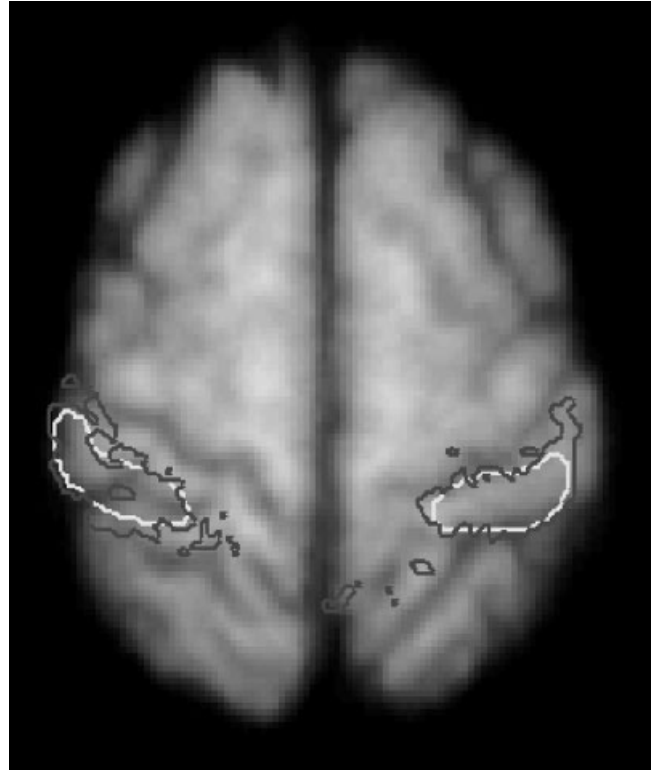

Figure 1.

Defining the VOI. Two volumes of interest (VOIs) representing the area 1 hand regions in the left and right hemispheres are overlaid onto the 38 subjects mean MRI. The black contours represent the cytoarchitectural probability map of area 1. The white contours represent the final VOIs after they have been physically shrunken to minimize contamination from neighbouring areas.

the combined results of two previous studies in which subjects were stimulated with (1) a rotating brush on the hand [Bodegard et al., 2000a] and (2) objects placed on the hand for discrimination [Bodegard et al., 2000b]. The remaining region superior to the hand region defined the lower body part and, likewise, the inferior region defined the face part.

A correlation analysis will show false-positive correlations around the border of an area if the area is taken directly from the probability map. This is due to limited spatial resolution in PET and the 6-mm Gaussian filtering applied to the PET images. To reduce such false-positive correlations, the volume used to represent each cytoarchitectural area in the probability map was shrunk so that voxels representing an area were minimally correlated with those of adjacent areas (Fig. 1). A probe area (e.g., area 1) was removed from the population map and the surrounding population map was made binary (values 1 for the remaining areas and

0 for the hole made by removing the probe area). This map was then filtered with a 6-mm Gaussian isotropic filter. These made the adjacent areas invade the probe area space. The VOI representing the probe area was then defined as all voxels having values < 0.5 giving a maximum of 15% correlation (corresponding to the tail of the Gaussian filter kernel) of voxel values with neighboring areas.

After the cytoarchitectural areas were somatotopically divided and shrunk this way, they were used as the volume of interest (VOI) for the correlation analysis.

Statistical analysis

Two types of analyses were performed. The first analysis was based on the correlations between all cytoarchitectural VOIs. A mean of the rCBF within the VOI in each scan was calculated and normalized by scaling with the global CBF. This rCBF value was further averaged across the three rest conditions for each subject such that the intersubject variance was taken into account. The covariance matrix of these subject mean VOI values was calculated for all cytoarchitectural VOIs, i.e., for areas 3a, 3b, 1, 2, 4a, 4p, 17, 18, 44, 45, Te 1.0, Te1.1, and Te 1.2. It should be noted that the size of the VOIs for area 3a foot sectors, 3a right face sector, and area 1 face sectors were only a few or no voxels (due to the shrinkage of the original cytoarchitectural volumes, see above). With the subdivisions of areas 3a, 3b, and 1, into face, hand, and lower body sectors, this amounted to a 32×32 matrix since the left and right hemisphere VOIs were treated as separate entities. From the covariance matrix, the correlation matrix was calculated. This was transformed to a matrix of Student t-values using the standard relation between the correlation coefficient, r, and t values. Assuming that no more than 100 of the matrix values would be significant, we set the threshold for significance at $P < 0.0005$ (Bonferroni correction). The data were scrutinized for outliers giving rise to false-positive (or negative) correlation in plots of the pair-wise voxel values (VOI A vs. VOI B) for each subject for any significant matrix element. We found 11 such outliers, clearly outside the contour ellipses of the remaining values in the plot. All 11 outliers originated from one subject, who was removed from the sample, such that the final sample consisted of 37 subjects (df = 30). Correlations with somatosensory areas 3a, 3b, 1, and 2 are reported in this study.

The other analysis concerned the correlations lying in the cortical space that was not represented by any statistically delimited cytoarchitectural areas, i.e., the cortex outside areas 3a, 3b, 1, 2, 4a, 4p, 17, 18, 44, 45, Te 1.0, Te1.1, and Te 1.2. For this analysis, we modeled the voxel values in the non-charted cortical space with a general linear model. Firstly, voxel values for each scan were normalized by scaling with the global mean CBF. Following this, voxel values were averaged for each subject across the three rest conditions. The resulting images were modeled using the general linear model (GLM) with subject and study effects as factors and the cytoarchitectural mean VOI values from the first analysis as covariate [Ledberg, 2000]. The cluster size corresponding to an estimated omnibus significance of $P < 0.05$ ($t = 3.3$) was estimated using 5,000 Monte Carlo simulations [Ledberg, 2000]. According to this significance limit, the t-image was thresholded at $t = 3.3$ with a minimum cluster size of 544 mm^3 voxels. We found no effect of study, i.e., the rest voxel values did not change significantly depending on which other conditions were tested in addition to rest.

In order to avoid spurious correlations in the rCBF between a probe cytoarchitectural region and the rest of the brain, we normalized the accumulated counts to a relative rCBF of 50. However, since the procedural normalization could be thought to leave some effect of the global blood flow on each VOI, we also specifically modeled the response in each voxel with the general linear model and the global brain counts as a covariate. We then calculated the residual from this model and used the residuals as input for the correlation analysis. Again, we introduced the global counts as a covariate. This latter procedure, however, gave the same correlation matrix, as did the simple normalization of the data. We concluded that the simple normalization sufficiently removed the effect of the global blood flow on the estimated correlations

Description of non-delineated brain regions

Since the whole cerebral cortex was not covered by the available probability map of cytoarchitectural areas, any statistically significant correlations to the premotor cortex (PM), supplementary motor area (SMA), interparietal area (IPA), or supramarginal gyrus were defined in the following way. The SMA was defined by Roland and Zilles [1998] as the cortex on the medial wall of the superior frontal gyrus immediately anterior to the medial part of motor area 4a and extending rostrally to the Talairach coordinate $y = +16$. The dorsal premotor cortex was defined as the cortex anterior to the dorsolateral part of motor area 4a and extending forward as long as the Talairach coordinate $y = +16$ [Roland and Zilles,

TABLE I. Correlation matrix of cytoarchitecturally defined VOIs*

Correlation matrix of cytoarchitecturally defined VOIs

	3a face left	3a hand left	3a hand right	3b face left	3b face right	3b foot right	3b hand left	3b hand right	1 foot left	1 foot right	1 hand left	1 hand right	2 left	2 right	4a left	4a right	4p left	4p right
3a face left		0.34	0.11	*0.56*	0.44	-0.10	0.16	0.19	-0.18	-0.25	-0.37	-0.18	0.02	-0.04	0.06	0.03	0.48	0.20
3a hand left	0.34		*0.71*	0.43	0.33	0.03	*0.71*	*0.61*	0.12	-0.20	-0.38	-0.29	0.26	0.30	0.43	0.23	0.46	0.41
3a hand right	0.11	*0.71*		0.35	0.30	0.21	0.51	*0.69*	0.01	-0.14	-0.26	-0.04	0.25	0.33	0.25	0.15	0.32	0.46
3b face left	*0.56*	0.43	0.35		*0.82*	0.09	0.43	*0.55*	0.12	0.06	0.14	0.24	0.06	0.34	0.12	0.14	0.11	0.15
3b face right	0.44	0.33	0.30	*0.82*		0.08	0.45	0.52	-0.06	-0.05	0.00	0.06	0.09	0.30	0.10	0.16	-0.03	-0.02
3b foot right	-0.10	0.03	0.21	0.09	0.08		0.16	0.38	0.32	0.39	0.15	0.16	0.20	0.28	0.17	0.42	-0.21	-0.02
3b hand left	0.16	*0.71*	0.51	0.43	0.45	0.16		*0.75*	0.01	-0.21	-0.14	-0.26	*0.64*	*0.62*	*0.58*	0.32	0.29	0.40
3b hand right	0.19	*0.61*	*0.69*	*0.55*	0.52	0.38	*0.75*		0.17	0.12	-0.04	0.14	*0.55*	*0.67*	0.45	0.33	0.25	0.34
1 foot left	-0.18	0.12	0.01	0.12	-0.06	0.32	0.01	0.17		*0.66*	0.46	0.31	0.17	0.15	0.51	*0.57*	-0.13	0.12
1 foot right	-0.25	-0.20	-0.14	0.06	-0.05	0.39	-0.21	0.12	*0.66*		0.53	0.54	0.06	0.13	0.05	0.32	-0.31	-0.19
1 hand left	-0.37	-0.38	-0.26	0.14	0.00	0.15	-0.14	-0.04	0.46	0.53		*0.68*	-0.05	0.19	-0.09	0.05	-0.46	-0.22
1 hand right	-0.18	-0.29	-0.04	0.24	0.06	0.16	-0.26	0.14	0.31	0.54	*0.68*		-0.26	0.24	-0.29	-0.11	-0.39	-0.31
2 left	0.02	0.26	0.25	0.06	0.09	0.20	*0.64*	*0.55*	0.17	0.06	-0.05	-0.26		0.49	*0.66*	0.50	0.32	0.45
2 right	-0.04	0.30	0.33	0.34	0.30	0.28	*0.62*	*0.67*	0.15	0.13	0.19	0.24	0.49		0.35	0.25	-0.11	0.12
4a left	0.06	0.43	0.25	0.12	0.10	0.17	*0.58*	0.45	0.51	0.05	-0.09	-0.29	*0.66*	0.35		*0.77*	0.36	*0.58*
4a right	0.03	0.23	0.15	0.14	0.16	0.42	0.32	0.33	*0.57*	0.32	0.05	-0.11	0.50	0.25	*0.77*		0.17	0.34
4p left	0.48	0.46	0.32	0.11	-0.03	-0.21	0.29	0.25	-0.13	-0.31	-0.46	-0.39	0.32	-0.11	0.36	0.17		*0.65*
4p_right	0.20	0.41	0.46	0.15	-0.02	-0.02	0.40	0.34	0.12	-0.19	-0.22	-0.31	0.45	0.12	*0.58*	0.34	*0.65*	

* Correlation matrix. The VOIs, representing areas 3a, 3b, and 1 (divided into face, hand, and foot sectors) and areas 2, 4a and 4p were tested for correlations. The statistical significance was Bonferroni corrected for 100 tests, r-values >0.55 were statistically significant ($P < 0.05$ after Bonferroni corrections for multiple tests on the matrix cells). Significant correlations appear in bold. Correlations between areas were compared with the known connectivity in monkeys. Bold frames denote areas that correlated and are known to be connected in the macaque. Shading denotes areas that did not correlate but are connected in monkeys.

1996b]. The ventral premotor area (PMv) was defined as the cortex anterior to area 4a and posterior to cytoarchitectural area 44. From our preliminary results, the anterior limitation of either the dorsal of the ventral premotor areas PMd and PMv is roughly y = 12 [Ramnani et al., 2002]. The putative somatosensory association area IPA was defined as in Roland and Zilles [1998], as the cortex lining the anterior portion of the intraparietal sulcus and consistently activated in a previous study [Bodegard et al., 2000b]. This area is abutting the posterior border of cytoarchitectural area 2. The supramarginal gyrus, containing a putative or several putative somatosensory areas, then comprised the cortex that was inferior and lateral to the IPA, posterior to area 2 and superior to the lateral sulcus. The posterior border of the putative somatosensory cortex in the supramarginal gyrus is not known.

RESULTS

All subjects included in this study reported that they were not disturbed or distracted by any events during the rest state scans included for analysis.

As explained in *Subjects and Methods*, the probe VOIs of the foot regions and right face region of area 3a, and area 1 face regions were too small to be represented. Therefore, these somatotopic regions are not reported in this study.

Correlations among somatosensory and motor areas

The statistically significant correlations among the cytoarchitecturally delineated somatosensory and motor areas are shown in the correlation matrix, Table I.

The somatotopical region of one area is often correlated with the somatotopical counterpart of another somatosensory area. For example, the face sector of area 3a was correlated with the face sector of area 3b and the hand sector of area 3a with the hand sector of area 3b (Table I). In addition, the hand sectors of area 3b and area 2 were correlated. Surprisingly, the somatotopical sector in one hemisphere was also correlated with that in the other hemisphere. For example, the hand sector of area 3b in the left hemisphere was correlated with the hand sector in the right hemisphere and vice versa, and the hand sectors of area 1 were mutually correlated (Table I).

In the left hemisphere, areas 3b, 1, and 2 were correlated with motor area 4a (Table I). As apparent from Table I, several areas known to be connected in the macaques were not found correlated in their rCBF. Apart from correlations between area 3a hand sector and the auditory area Te 1.1 in the left hemisphere, there were no other statistically significant correlations.

Correlations between somatosensory areas and non-delineated brain regions

A summary of these results is displayed in Figure 2. This analysis is more descriptive as there were no probability maps of cytoarchitectural areas covering this space. Overlaps of correlated clusters and grey matter with a volume larger than 544 mm^3 were, from the statistical analysis, statistically significant ($P < 0.05$ corrected for multiple comparisons; Fig. 2).

The rCBF in the hand sectors of area 3a correlated with the rCBF of the PMd (Fig. 2) and the cortex lining the rostral part of the superior frontal sulcus in the left hemisphere (Fig. 2). The face sector of area 3a left correlated with the right SMA (Fig. 2).

The hand sectors of area 3b, similarly with the hand sector of area 3a, correlated with the PMd and with an additional area located just caudally to Te 1.1 in the planum temporale (Fig. 2). The face sectors of area 3b had numerous correlations. These included the area located just caudally to Te 1.1 in the planum temporale. No regions correlated with the lower body section of area 3b.

The hand sector of area 1 in the left hemisphere correlated with the right middle frontal gyrus, IPA, left ASM areas, and an area in the posterior half of the right orbitofrontal cortex (Fig. 2). The hand sector of area 1 in the right hemisphere correlated with the ipsilateral PMd. Area 1 lower-body sectors only in the left hemisphere correlated with motor areas (Fig. 2), and both correlated with the anterior part of the superior parietal lobule (Fig. 2). The face sector of area 1 in the right hemisphere and areas 2 on the left and right side did not show any significant positive correlations with other areas. Table II is included for comparison with macaque connectivity.

Negative correlations

The face sector of area 3b was negatively correlated with area 18, and the hand sectors of area 1 were negatively correlated with area 4p in the left hemisphere. Each of the somatosensory cytoarchitectural areas 3a, 3b, 1, and 2 had their rCBF negatively correlated with the rCBF of a larger part of the anterior ventral and dorsal thalamus. This part comprises the AV and AM nuclei of thalamus according to the stereotaxic atlas of Schaltenbrand and Bailey [1959].

Some common trends were noted from the negative correlations. The rCBF of the hand sectors of areas 3a and 3b were negatively correlated with the rCBF in the superior part of the middle frontal gyrus, and often also with the lateral part of the posterior lobule of the cerebellum. The rCBF of several sectors in areas 3a, 3b, and 1 were negatively correlated with regions in the posterior part of the brain often activated by visual stimuli such as the posterior part of the superior parietal lobule, the precuneus and the inferior temporal cortex.

DISCUSSION

The general pattern of correlations between somatosensory areas was such that the hand sector of an area was correlated with the hand sector of other somatosensory areas in the same hemisphere. Similarly, face sectors were correlated with face sectors but not with hand or lower body sectors. Surprisingly the somatotopical sectors of areas 3a, 3b, and 1, were correlated with their somatotopical counterparts in the other hemisphere. In addition, somatosensory areas 3a, 3b, and 1, correlated with the PMd and areas 3b and 1 correlated with area 4a. Furthermore, area 1 correlated with putative somatosensory areas in the parietal lobules, but surprisingly area 2 had no such correlations. Finally, the somatosensory areas had positive correlations with different prefrontal and temporal areas and negative correlations with the anterior thalamus and visual areas.

To define the VOI, each cytoarchitecturally defined area from the probability map was shrunk (see *Subjects and Methods*). This procedure was performed to minimize rCBF signal contamination from neighbour-

VOI correlations with brain regions outside of the cytoarchitecturally delineated areas

Area 3a hand
Superior frontal sulcus
L -22 28 28 1344 mm³
R   18 14 36   728 mm³
PMd
L -30 -12 34   696 mm³
L -24 -20 46   569 mm³
R   30   -8 34   760 mm³

Area 3a hand
Superior frontal sulcus
L -22 28 28 808 mm³
PMd
R   36   -4 38 784 mm³
Superior temporal gyrus
R   44 -32 14 704 mm³

Legend: area 3b (yellow), area 1 (teal), area 2 (red)

Area 3a face
SMA
L -22 2 32 880 mm³

Area 3b face
Inferior frontal gyrus
L -44 2 4 760 mm³

Area 3b face
Inferior temporal gyrus
R 58 -54 -10 1464 mm³
Occipital lobule
R   6 -88 -20 2904 mm³
Te 1.1
R 42 -20   4   712 mm³
Supramarginal gyrus
R 60 -38   18 2272 mm³

Area 3b hand
Superior temporal gyrus
R 46 -32 12 576 mm³
PMd
L -20 -22 50 816 mm³
R   20 -20 58 760 mm³

Area 3b hand
Superior temporal gyrus
R 46 -30 12 752 mm³
PMd
R 18 -20 56 1624 mm³
R 36   -4 36   832 mm³
L -24 -22 44   956 mm³

Area 1 hand
Middle frontal gyrus
R -44   8 48   624 mm³
IPA
R 44 -38 54 1824 mm³
L -56 -50 34 1104 mm³
ASM
L -42 -68 40 1800 mm³
Orbitofrontal gyrus
R 22 26 -18   560 mm³

Area 1 Lower body
PMd
L -22 -20 64 2105 mm³
R   22 -20 64 1623 mm³
SMA
R   6 -18 64   638 mm³
Superior parietal lobule
L -24 -56 58 1537 mm³
R   18 -56 58   989 mm³
Anterior superior frontal gyrus
L   -6 26 50   600 mm³

Area 1 hand
PMd
R 48 -4 48 576 mm³

Area 1 lower body
Superior parietal lobule
L -32 -70 44 1176 mm³
Parietal lobule
R   40 -52 48 1072 mm³
Supramarginal gyrus
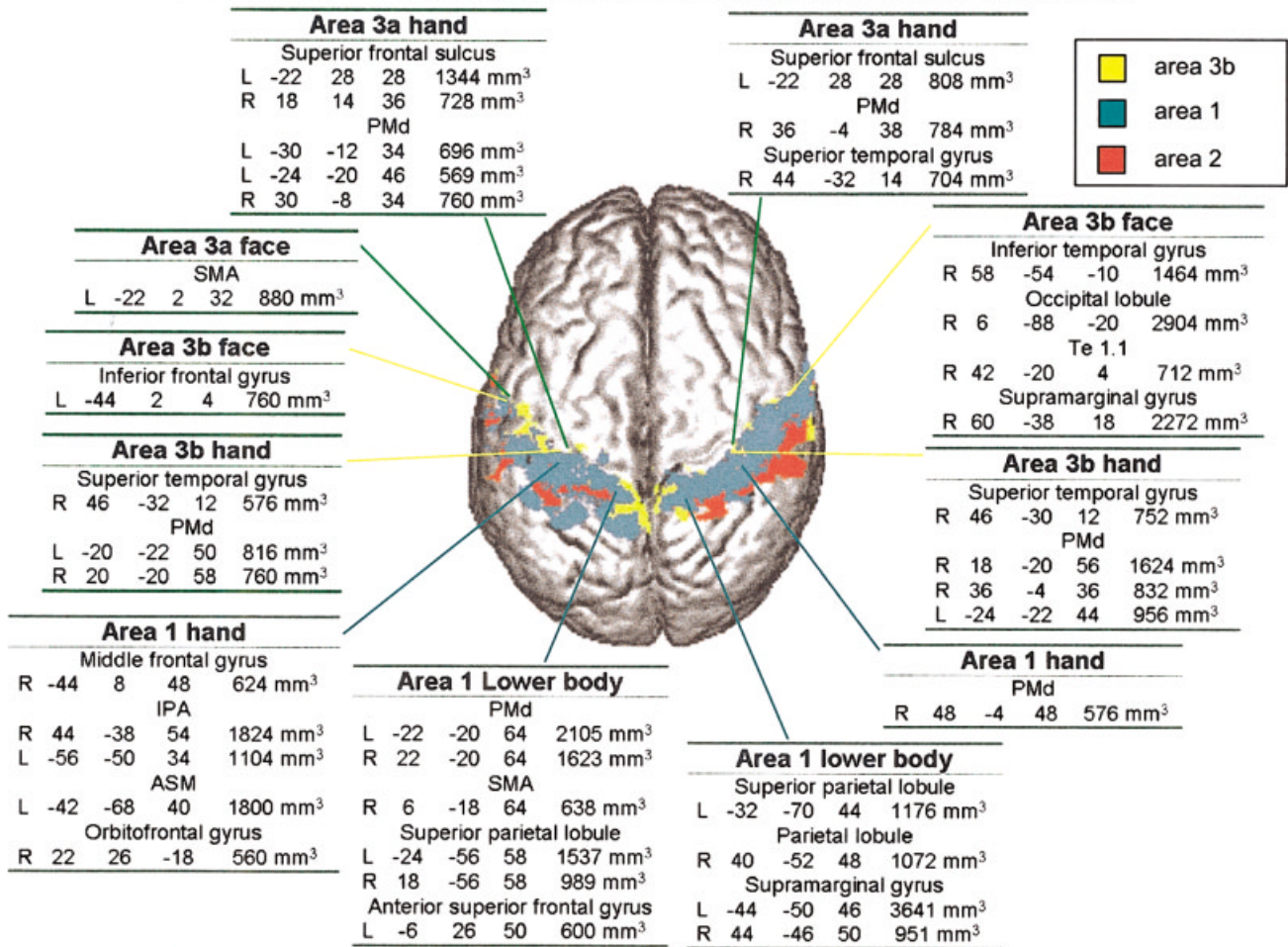L -44 -50 46 3641 mm³
R   44 -46 50   951 mm³

Figure 2.

Correlations between the cytoarchitectural VOI and brain regions that were not cytoarchitecturally delineated. The remaining voxels of the brain, undefined by cytoarchitectural delineation, were searched for correlations with each VOI. Correlating brain regions were thresholded at $t = 3.3$ and clustered at 544 mm². For each VOIs representing areas 3a, 3b, and 1 (face, hand, and foot regions), is a table listing the correlated brain regions and their Talairach coordinates.

ing voxels due to the limited spatial resolution of PET images. Doing so, the VOI became smaller than the volume defined cytoarchitecturally. In some cases, the VOI became too small that either there were no voxels remaining to represent a somatotopic subdivision of an area, or there were too few voxels to provide a reliable estimate of the mean rCBF within the VOI of that somatotopic region. In particular, the lower body sectors and somatotopical sectors of area 3a were poorly represented. Shrinking the VOI appeared to be an effective way of minimizing rCBF signal contamination from neighbouring voxels belonging to adjacent areas since we found no correlations between the rCBF in areas 4p and 3a, 4p and 3b, or between areas 1 and 2.

Probability maps of cytoarchitectural areas from 10 postmortem human brains were used to statistically estimate the location of an area over the population of subjects used in this experiment. Due to between subject variance, it is possible that the voxels within a defined area of the probability map may not exclusively represent that area in the brain, but rather a mixture of the defined area and adjacent areas when one considers a population of 10 brains [Geyer et al., 1996; Roland and Zilles, 1996b]. Since the voxels were allocated to the area represented by most brains, the

TABLE II. Connectivity of somatosensory area 3a, 3b, 1, and 2 with other somatosensory areas in the Macaque*

	VPL left	VPL right	Area 5 left	Area 5 right	AIP left	AIP right	PO left	PO right	SII left	SII right	PM left	PM right	SMA left	SMA right
Area 3a left	+								+	+				
Area 3a right		+							+	+				
Area 3b left	+						+		+	+				
Area 3b right		+						+	+	+				
Area 1 left	+				+	?	+		+	+				
Area 1 right		+			?	+		+	+	+				
Area 2 left	+		+	+	+	?	+	?	+	+	+		+	
Area 2 right		+	+	+	?	+	?	+	+	+		+		+

* For comparison with Figure 2. +, connection exists in macaques based on several reports; ?, direct anatomical connections based on one report; shading, a correlation.

probability map is still the best estimate for locating an area, given the restriction that neighboring areas should abut each other. The correspondence between the probability map and the PET images was examined as described in Materials and Methods. Still, the VOIs used in this experiment to represent the cytoarchitectural areas should be taken as no more than the best estimates of the locations of these areas.

For areas 3a, 3b, 1, 2, and motor areas 4a, 4p, the laminar receptor densities, and cell body densities are very similar in the two species [Geyer et al., 1999; Grefkes et al., 2001; Zilles et al., 1995]. For other areas, the homologues are at present less certain, especially posterior to area 2 [Zilles and Palomero-Gallagher, 2001]. As anatomical connections are important factors in defining cortical areas together with cytoarchitectural characteristics, the inter correlations of the areas 4a, 4p, 3a, 3b, 1, and 2 can at best be interpreted as either reflecting or not reflecting the anatomical connectivity under the (relatively well-determined) assumptions of homology between macaques and humans. It is possible, but less well documented [Eickhoff et al., 2002] that the parietal operculum is another region of homology between the two species.

Based on this micro-structural evidence, we tested the hypothesis that the pattern of correlations among brain regions is similar to that of the established monkey connectivity.

Correlations of somatosensory areas with other somatosensory areas

One of the main findings was that the somatotopical regions of area 3a were connected with the corresponding somatotopical regions of area 3b. Thus, face, hand, and lower body somatotopy was preserved in the correlations. This correlation pattern matches closely that of the connections between areas 3a and 3b reported in macaques [Burton and Fabri, 1995; Iwamura et al., 1980; Jones and Powell, 1969; Krubitzer and Kaas, 1990; Pons and Kaas, 1986].

Correlations of area 3b hand with area 2 match with macaque connectivity [Burton and Fabri, 1995]. In contrast with macaque connectivity, however, there were no statistically significant correlations in rCBF between area 3b and 1, or areas 1 and 2. Area 1 did correlate with the blood flow in the functionally delimited region IPA [Bodegard et al., 2001; Roland and Zilles, 1998].

In macaques, area 2 is said to project to areas 5 and somatosensory areas in the parietal operculum (Pons et al., 1985; Pons and Kaas, 1985). Area 5 was not included in our collection of cytoarchitectural areas, but preliminary investigations suggest that this area is located in the superior parietal lobule, in a region outside the area correlated with the foot sectors of area 1. Similarly, cytoarchitectural areas 3a, 3b, 1, and 2 did not show any statistically significant correlations with the parietal operculum. Thus, the secondary somatosensory area and related areas in the parietal operculum of the monkey that are well documented to be connected to areas 3a, 3b, 1, and 2 in the monkey [Burton et al., 1995; Friedman et al., 1980; Krubitzer and Kaas, 1990; Manzoni et al., 1986], were not evident from this study.

Area 7b in the monkey is located near the parietal operculum. Both left hemisphere area 1 lower body and area 3b face regions correlated with a field in the supramarginal gyrus. It is impossible, however, to determine whether this field in the supramarginal gyrus corresponds to area 7b since the inferior parietal lobule is organized differently in macaques and humans [Brodmann, 1909; Zilles and Palomero-Gallagher, 2001].

In macaques, area 2 has abundant callosal connections with area 2 on the contralateral side, and the face and trunk regions of areas 3a, 3b, and 1 have callosal connections [Killackey et al., 1983; Pandya and Vignolo, 1971]. Correlations between left and right area 2 regions were absent. Although we found inter-hemispheric correlations of the face and trunk/foot parts of areas 3b, 1, we also found inter-hemispheric correlations of the hand sectors of areas 3a, 3b, and 1. The latter is in conflict with observations in macaques that the hand parts of these areas have no callosal connections [Killackey et al., 1983; Pandya and Vignolo, 1971].

Homologies and analogies in the organization of the monkey posterior parietal cortex and the human posterior parietal cortex are questionable [Zilles and Palomero-Gallagher, 2001]. The area we have called IPA, based on functional criteria [Bodegard et al., 2001; Roland and Zilles, 1998], is distinct from the monkey anterior interparietal area (AIP) [Gallese et al., 1994; Sakata et al., 1995; Taira et al., 1990], since the IPA is active when the subjects have their eyes closed and are not performing any manipulations with their hands. Similarly, area 5 of humans, which according to our preliminary studies is located rather medially in the superior parietal lobule, is probably distinct from the area 5 lining the medial bank of the intraparietal sulcus in monkeys. Furthermore, area 2 in humans does not abut area 5 in the anterior part of the intraparietal sulcus [Grefkes et al., 2001]. Finally, humans have areas 40 and 39 that do not exist in monkeys [Brodmann, 1909; Vogt and Vogt, 1926; von Economo and Koskinas, 1925]. Area 2 had no correlations with any of the putative somatosensory areas in the posterior parietal cortex, in contrast to area 1, which had correlations with IPA as well as the functional delimited area ASM in the anterior part of the supramarginal gyrus [Bodegard et al., 2001].

Thus, we found some correlations between areas 3a, 3b, 1, and 2 that were consistent with the connectivity of these areas in monkeys. The results, however, failed to demonstrate correlations between these areas and SII and other areas in the parietal operculum, and failed to show correlations between areas 3b and 1, 3a and 2, and 1 and 2, i.e., between areas that are strongly connected in the macaque.

Correlations of area 3a, 3b, 1, and 2 with motor areas

Area 1 correlated with area 4a. Whether there are connections between area 1 and 4a in the macaque is considered controversial, although sparse connections have been described [Burton and Fabri, 1995; Kunzle, 1978; Stepniewska et al., 1993]. Likewise, that area 2 rCBF correlated with the rCBF of areas 4a and 4p is also controversial; however, projections from area 2 to 4a, 4p in the macaque have been reported [Ghosh et al., 1987; Jones et al., 1978; Pons and Kaas, 1986]. The correlation matrix, however, does not fit with the somatosensory areas reported to be most connected to areas 4a and 4p in macaques, i.e., areas 3a, 3b [Darian-Smith et al., 1990; Huerta and Pons, 1990; Jones et al., 1978; Krubitzer and Kaas, 1990; Pons and Kaas, 1986; Stepniewska et al., 1993]. Connections from area 3a to area 4 have been described [Darian-Smith et al., 1990; Huerta and Pons, 1990; Krubitzer and Kaas, 1990; Stepniewska et al., 1993] and that projections from area 3 reach both the rostral primary motor cortex, which in humans is likely to be in area 4a, as well as the caudal portion, which in humans is likely to be in area 4p.

The rCBF in area 3a was correlated with the rCBF in the supplementary motor area (SMA). In macaques, no connections have been reported from area 3a to the SMA [Huerta and Pons, 1990; Luppino et al., 1993; McGuire et al., 1991a], although projections from the SMA to area 3a have been described [Darian-Smith et al., 1990]. Such connections have also been described in the Marmoset [Huffman and Krubitzer, 2001].

Discrepant from the areas involved in macaque connectivity, was our finding that areas 3a, 3b, and 1 were strongly correlated with the dorsal pre-motor cortex (PMd). Also, there were no correlations between area 2 and the PM and SMA. In the macaque, projections from area 2 to PMd have been reported [Barbas and Pandya, 1987; Ghosh and Gattera, 1995; Jones et al., 1978; Vogt and Pandya, 1978], although, other investigators have described very sparse or no connections between area 2 and PMd [Ghosh and Gattera, 1995; McGuire et al., 1991b; Pons and Kaas, 1986].

Again, we found some correlations between somatosensory areas 3a, 3b, 1, and 2, which were supported by similar connections in the macaque, but failed to demonstrate correlations that were expected from macaque connectivity. In addition, we found correlations with the PMd, which have no counterparts in macaque connectivity.

Correlations between somatosensory areas and other regions

Areas 3a, 3b, and 1 correlated with the cortex lining the anterior part of the superior frontal sulcus and the

orbitofrontal cortex. Neural connections between areas 3a, 3b, and 1 and these prefrontal areas in the monkey are unsupported. Similarly, there were correlations between areas 3a, 3b, the primary auditory area Te 1.1, and the adjacent part of the planum temporale, which are also unsupported by macaque connectivity.

Other explanations of the data

Although the positive correlations we found between area 3a, 3b, 1, and 2, mutually and with the remaining brain, in some aspects, were in accordance with the hypothesis of similar direct anatomical connectivity in humans and macaques, we found correlations in cases in which no direct connections exist in the macaque and we failed to demonstrate correlations in cases of direct connectivity. These failures to find correlations, where strong connectivity should be expected, did not arise because our criteria for statistically significance were too conservative. For example, if one looks at the correlations between area 3a and area 2 or between area 1 and 2 in Table I, the correlation coefficient r is rather low and not near significance. One explanation of the several failures of this kind might come from the observations that only a small part of the connectivity at any place in the cerebral cortex is extrinsic, i.e., between cortical areas. By far, most of the connections are intrinsic, between neurons within the cortex [Rockland and Pandya, 1979; Wiser and Callaway, 1996; Yukie and Iwai, 1985]. It is likely that spontaneous activity exists in local cortical fields as thalamo-cortico-thalamic activity and local intrinsic cortical action potentials, without this giving rise to any but sparse cortico-cortical action potential activity [Roland, 2002]. This might also be the reason why Xiong et al. [1998], similar to our results, also found correlations among motor areas, which has a counterpart in macaque connectivity, but also failed to detect all direct connections between motor areas from the macaque connectivity.

Negative correlations

We found negative correlations with several areas, including the posterior parts of the superior parietal lobules, precuneus, the inferior temporal cortex, fusiforme gyri, posterior cerebellum, and the occipital lobe. As all cortico-cortical connections are thought to be glutamatergic and excitatory [Ottersen and Storm-Mathisen, 1986; Storm-Mathisen and Fonnum, 1972], one cannot explain these negative correlations by cortico-cortical connectivity alone, notwithstanding that

no connections exist between areas 3a, 3b, 1, 2, and the visual cortex in other primates.

The visual areas are regions that often decrease their rCBF during somatosensory tasks [Haxby et al., 1994; Kawashima et al., 1995], an effect that is thought to be of subcortical origin.

The cortical areas that correlated negatively with the rCBF in areas 3a, 3b, 1, and 2, do not have direct cortico-cortical connections in the macaque, with the exception of area 4p.

The rCBF of the lateral parts of the posterior lobule of the cerebellum were consistently negatively correlated with areas 3b, 1, and 2. As the cortico-pontine-cerebellar input to the cerebellum target the inhibitory basket, stellate, Golgi, and Purkinje neurons (by the parallel fibres), this might be the reason for this negative rCBF correlation. Thus, despite the synapses on the granule cells being excitatory, the overall effect may be a reduction on cerebellar excitation at rest. However, we have no explanation why this effect is located to the posterior lobe only.

The cortico-thalamic projections, from a given cortical area, are said to outnumber the thalamo-cortical projections by as much as ten to one [Sherman and Koch, 1986]. It has been a matter of long-standing controversy whether the effect of the cortico-thalamic fibres on the thalamus would be excitatory or inhibitory at the thalamic target nucleus [Llinas and Pare, 1997]. Thus, there is a possibility that the correlations in some case might reflect indirect connectivity, in this case via the thalamus. The negative correlations with the AV and AM thalamic nuclei may be an example of cortico-thalamic connectivity to inhibitory neurons [Llinas and Pare, 1997].

In any case, neither of these explanations is valid for our finding of a correlation between the hand sectors of the right and left hemispheres for areas 3a, 3b, and 1. Correlations between an area and its homologue in the other hemisphere are, however, consistent with previous correlations also between hand sectors in sensory and motor cortex obtained with PET and fMRI during rest [Cordes et al., 2001; Lowe et al., 1998; Xiong et al., 1999]. One cannot, then, exclude the possibility that the rest state may induce correlations, i.e., the instruction to "lie motionless, to not pay any attention to anything in particular and not to think, but have it black in front of the mind's eye."

CONCLUSIONS

We used an unbiased method to examine the correlations in rCBF of somatosensory areas 3a, 3b, 1, and 2

under the main hypothesis that the rCBF correlations would reflect the connectivity of the homologous areas in other primates. We found three types of results: correlations that match with macaque connectivity, correlations with no counterpart in macaque connectivity, and lack of correlations between areas clearly connected to somatosensory areas in macaques. On these grounds, the main hypothesis is refuted in two instances. The correlations of rCBF among somatosensory areas, between somatosensory areas and other cortical areas, in humans at rest can only partly rely on direct cortico-cortical connections. For theoretical reasons, this might not be expected, as the majority of the neuronal connections in the cortex are local intracortical connections. Other factors, such as cortico-thalamo-cortical mechanism and the rest state per se, may influence the pattern of correlations observed among cortical areas.

ACKNOWLEDGMENTS

REFERENCES

Amunts K, Schleicher A, Burgel U, Mohlberg H, Uylings HB, Zilles K (1999): Broca's region revisited: cytoarchitecture and intersubject variability. J Comp Neurol 412:319–341.

Amunts K, Malikovic A, Mohlberg H, Schormann T, Zilles K (2000): Brodmann's areas 17 and 18 brought into stereotaxic space—where and how variable? Neuroimage 11:66–84.

Barbas H, Pandya DN (1987): Architecture and frontal cortical connections of the premotor cortex (area 6) in the rhesus monkey. J Comp Neurol 256:211–228.

Bergström M, Boethius J, Eriksson L, Greitz T, Ribbe T, Widen L (1981): Head fixation device for reproducible position alignment in transmission CT and positron emission tomography. J Comput Assist Tomogr 5:136–141.

Biswal B, Yetkin FZ, Haughton VM, Hyde JS (1995): Functional connectivity in the motor cortex of resting human brain using echo-planar MRI. Magn Reson Med 34:537–541.

Bodegard A, Geyer S, Grefkes C, Zilles K, Roland PE (2001): Hierarchical processing of tactile shape in the human brain. Neuron 31:317–328.

Bodegard A, Geyer S, Naito E, Zilles K, Roland PE (2000a): Somatosensory areas in man activated by moving stimuli: cytoarchitectonic mapping and PET. Neuroreport 11:187–191.

Bodegard A, Ledberg A, Geyer S, Naito E, Zilles K, Roland PE (2000b): Object shape differences reflected by somatosensory cortical activation. J Neurosci (online) 20:RC51.

Brodmann K (1909): Vergleichende Lokalisationslehre der Grosshirnrinde in Ihren Prinzipien Dargestellt Auf Grund Des Zellenbaues. Barth.

Burkhalter A, Bernardo KL, Charles V (1993): Development of local circuits in human visual cortex. J Neurosci 13:1916–1931.

Burton H, Fabri M (1995): Ipsilateral intracortical connections of physiologically defined cutaneous representations in areas 3b and 1 of macaque monkeys: projections in the vicinity of the central sulcus. J Comp Neurol 355:508–538.

Burton H, Fabri M, Alloway K (1995): Cortical areas within the lateral sulcus connected to cutaneous representations in areas 3b and 1: a revised interpretation of the second somatosensory area in macaque monkeys. J Comp Neurol 355:539–562.

Cordes D, Haughton VM, Arfanakis K, Carew JD, Turski PA, Moritz CH, Quigley MA, Meyerand ME (2001): Frequencies contributing to functional connectivity in the cerebral cortex in "resting-state" data. AJNR Am J Neuroradiol 22:1326–1333.

Darian-Smith C, Darian-Smith I, Cheema SS (1990): Thalamic projections to sensorimotor cortex in the macaque monkey: use of multiple retrograde fluorescent tracers. J Comp Neurol 299:17–46.

Eickhoff S, Geyer S, Amunts K, Mohlberg H, Zilles K (2002): Cytoarchitectonic analysis and stereotaxic map of the human secondary somatosensory cortex region. Neuroimage 17(Suppl. 8): 792.

Friedman DP, Jones EG, Burton H (1980): Representation pattern in the second somatic sensory area of the monkey cerebral cortex. J Comp Neurol 192:21–41.

Friston KJ (1994): Functional and effective connectivity in neuroimaging: a synthesis. Hum Brain Mapp 2:56–78.

Gallese V, Murata A, Kaseda M, Niki N, Sakata H (1994): Deficit of hand preshaping after muscimol injection in monkey parietal cortex. Neuroreport 5:1525–1529.

Galuske RA, Schlote W, Bratzke H, Singer W (2000): Interhemispheric asymmetries of the modular structure in human temporal cortex [see comments]. Science 289:1946–1949.

Geyer S, Ledberg A, Schleicher A, Kinomura S, Schormann T, Burgel U, Klingberg T, Larsson J, Zilles K, Roland PE (1996): Two different areas within the primary motor cortex of man. Nature 382:805–807.

Geyer S, Schleicher A, Zilles K (1999): Areas 3a, 3b, and 1 of human primary somatosensory cortex. Neuroimage 10:63–83.

Ghosh S, Gattera R (1995): A comparison of the ipsilateral cortical projections to the dorsal and ventral subdivisions of the macaque premotor cortex. Somatosens Mot Res 12:359–378.

Ghosh S, Brinkman C, Porter R (1987): A quantitative study of the distribution of neurons projecting to the precentral motor cortex in the monkey (M. fascicularis). J Comp Neurol 259:424–444.

Grefkes C, Geyer S, Schormann T, Roland P, Zilles K (2001): Human somatosensory area 2: observer-independent cytoarchitectonic mapping, interindividual variability, and population map. Neuroimage 14:617–631.

Hadjikhani N, Roland PE (1998): Cross-modal transfer of information between the tactile and the visual representations in the human brain: A positron emission tomographic study. J Neurosci 18:1072–1084.

Haxby JV, Horwitz B, Ungerleider LG, Maisog JM, Pietrini P, Grady CL (1994): The functional organization of human extrastriate cortex: a PET-rCBF study of selective attention to faces and locations. J Neurosci 14:6336–6353.

Horwitz B (1994): Data analysis paradigms for metabolic + flow data combining neural modeling and functional neuroimaging. Hum Brain Mapp 2:112–122.

Horwitz B, Duara R, Rapoport SI (1984): Intercorrelations of glucose metabolic rates between brain regions: application to healthy

males in a state of reduced sensory input. J Cereb Blood Flow Metab 4:484–499.

Huerta MF, Pons TP (1990): Primary motor cortex receives input from area 3a in macaques. Brain Res 537:367–371.

Huffman KJ, Krubitzer L (2001): Area 3a: topographic organization and cortical connections in marmoset monkeys. Cereb Cortex 11:849–867.

Iwamura Y, Tanaka M, Hikosaka O (1980): Overlapping representation of fingers in the somatosensory cortex (area 2) of the conscious monkey. Brain Res 197:516–520.

Jones EG, Powell TP (1969): Connexions of the somatic sensory cortex of the rhesus monkey. I. Ipsilateral cortical connexions. Brain 92:477–502.

Jones EG, Coulter JD, Hendry SH (1978): Intracortical connectivity of architectonic fields in the somatic sensory, motor and parietal cortex of monkeys. J Comp Neurol 181:291–347.

Kawashima R, O'Sullivan BT, Roland PE (1995): Positron-emission tomography studies of cross-modality inhibition in selective attentional tasks: closing the "mind's eye." Proc Natl Acad Sci U S A 92:5969–5972.

Killackey HP, Gould HJd, Cusick CG, Pons TP, Kaas JH (1983): The relation of corpus callosum connections to architectonic fields and body surface maps in sensorimotor cortex of new and old world monkeys. J Comp Neurol 219:384–419.

Krubitzer LA, Kaas JH (1990): The organization and connections of somatosensory cortex in marmosets. J Neurosci 10:952–974.

Kunzle H (1978): An autoradiographic analysis of the efferent connections from premotor and adjacent prefrontal regions (areas 6 and 9) in macaca fascicularis. Brain Behav Evol 15:185–234.

Larsen B, Skinhoj E, Lassen NA (1978): Variations in regional cortical blood flow in the right and left hemispheres during automatic speech. Brain 101:193–209.

Ledberg A (2000): Robust estimation of the probabilities of 3-D clusters in functional brain images: application to PET data. Hum Brain Mapp 9:143–155.

Llinas RR (1988): The intrinsic electrophysiological properties of mammalian neurons: insights into central nervous system function. Science 242:1654–1664.

Llinas R, Pare D (1997): Coherent oscillations in the specific and nonspecific thalamocortical networks and their role in cognition. In: Steriade M, Jones EG, McCormick D, Editors. Thalamus. p 501–516. New York: Elsevier.

Lowe MJ, Mock BJ, Sorenson JA (1998): Functional connectivity in single and multislice echoplanar imaging using resting-state fluctuations. Neuroimage 7:119–132.

Luppino G, Matelli M, Camarda R, Rizzolatti G (1993): Corticocortical connections of area F3 (SMA-proper) and area F6 (pre-SMA) in the macaque monkey. J Comp Neurol 338:114–140.

Manzoni T, Conti F, Fabri M (1986): Callosal projections from area SII to SI in monkeys: anatomical organization and comparison with association projections. J Comp Neurol 252:245–263.

McGuire PK, Bates JF, Goldman-Rakic PS (1991a): Interhemispheric integration: I. Symmetry and convergence of the corticocortical connections of the left and the right principal sulcus (PS) and the left and the right supplementary motor area (SMA) in the rhesus monkey. Cereb Cortex 1:390–407.

McGuire PK, Bates JF, Goldman-Rakic PS (1991b): Interhemispheric integration: II. Symmetry and convergence of the corticostriatal projections of the left and the right principal sulcus (PS) and the left and the right supplementary motor area (SMA) of the rhesus monkey. Cereb Cortex 1:408–417.

Meyer E (1989): Simultaneous correction for tracer arrival delay and dispersion in CBF measurements by the $H_2^{15}O$ autoradiographic method and dynamic PET. J Nucl Med 30:1069–1078.

Morosan P, Rademacher J, Schleicher A, Amunts K, Schormann T, Zilles K (2001): Human primary auditory cortex: cytoarchitectonic subdivisions and mapping into a spatial reference system. Neuroimage 13:684–701.

Oldfield RC (1971): The assessment and analysis of handedness: the Edinburgh inventory. Neuropsychologia 9:97–113.

Olesen J, Paulson OB, Lassen NA (1971): Regional cerebral blood flow in man determined by the initial slope of the clearance of intra-arterially injected 133Xe. Stroke 2:519–540.

Ottersen OP, Storm-Mathisen J (1986): Excitatory amino acid pathways in the brain. Adv Exp Med Biol 203:263–284.

Pandya DN, Vignolo LA (1971): Intra- and interhemispheric projections of the precentral, premotor and arcuate areas in the rhesus monkey. Brain Res 26:217–233.

Pons TP, Kaas JH (1985): Connections of area 2 of somatosensory cortex with the anterior pulvinar and subdivisions of the ventroposterior complex in macaque monkeys. J Comp Neurol 240:16–36.

Pons TP, Kaas JH (1986): Corticocortical connections of area 2 of somatosensory cortex in macaque monkeys: a correlative anatomical and electrophysiological study. J Comp Neurol 248:313–335.

Pons TP, Garraghty PE, Cusick CG, Kaas JH (1985): The somatotopic organization of area 2 in macaque monkeys. J Comp Neurol 241:445–466.

Ramnani N, Johnsen-Berg H, Geyer S, Mohlberg H, Smith S, Zilles K, Matthews P (2002): The human primary motor cortex: Probabilistic cytoarchitecture and function in MNI spaceq. Neuroimage 17(Suppl. 8):822.

Rockland KS, Pandya DN (1979): Laminar origins and terminations of cortical connections of the occipital lobe in the rhesus monkey. Brain Res 179:3–20.

Roland PE (2002): Dynamic depolarization fields in the cerebral cortex. Trends Neurosci 25:183–190.

Roland E, Larsen B (1976): Focal increase of cerebral blood flow during stereognostic testing in man. Arch Neurol 33:551–558.

Roland PE, Zilles K (1996a): Functions and structures of the motor cortices in humans. Curr Opin Neurobiol 6:773–781.

Roland PE, Zilles K (1996b): The developing European computerized human brain database for all imaging modalities. Neuroimage 4:S39–47.

Roland PE, Zilles K (1998): Structural divisions and functional fields in the human cerebral cortex. Brain Res Brain Res Rev 26:87–105.

Roland PE, Graufelds CJ, Wåhlin J, Ingelman L, Andersson M, Ledberg A, Pedersen J, Åkerman S, Dabringhaus A, Zilles K (1994): Human brain atlas: for high-resolution functional and anatomical mapping. Hum Brain Mapp 1:173–184.

Sakata H, Taira M, Murata A, Mine S (1995): Neural mechanisms of visual guidance of hand action in the parietal cortex of the monkey. Cereb Cortex 5:429–438.

Schaltenbrand G, Bailey P (1959): Introduction to stereotaxis, with an atlas of the human brain [German language]. Stuttgart: Thieme.

Schleicher A, Amunts K, Geyer S, Morosan P, Zilles K (1999): Observer-independent method for microstructural parcellation of cerebral cortex: a quantitative approach to cytoarchitectonics. Neuroimage 9:165–177.

Schormann T, Zilles K (1998): Three-dimensional linear and nonlinear transformations: an integration of light microscopical and MRI data. Hum Brain Mapp 6:339–347.

Sherman SM, Koch C (1986): The control of retinogeniculate transmission in the mammalian lateral geniculate nucleus. Exp Brain Res 63:1–20.

Stepniewska I, Preuss TM, Kaas JH (1993): Architectonics, somatotopic organization, and ipsilateral cortical connections of the primary motor area (M1) of owl monkeys. J Comp Neurol 330:238–271.

Steriade M, McCormick DA, Sejnowski TJ (1993): Thalamocortical oscillations in the sleeping and aroused brain. Science 262:679–685.

Storm-Mathisen J, Fonnum F (1972): Localization of transmitter candidates in the hippocampal region. Prog Brain Res 36:41–58.

Taira M, Mine S, Georgopoulos AP, Murata A, Sakata H (1990): Parietal cortex neurons of the monkey related to the visual guidance of hand movement. Exp Brain Res 83:29–36.

Vogt BA, Pandya DN (1978): Cortico-cortical connections of somatic sensory cortex (areas 3, 1 and 2) in the rhesus monkey. J Comp Neurol 177:179–191.

Vogt C, Vogt O (1926): Die vergleichend-architektonische und vergleichend-reizphysiologische Felderung der Großhirnrinde unter besonderer Berucksichtigung der menschlichen. Naturwissenschaften 14:1190–1194.

von Economo C, Koskinas GN (1925): Die cytoarchitektonik der hirnrinde des erwachsenen menschen. Wien: Springer.

Wiser AK, Callaway EM (1996): Contributions of individual layer 6 pyramidal neurons to local circuitry in macaque primary visual cortex. J Neurosci 16:2724–2739.

Woods R, Cherry S, Mazziotta J (1992): Rapid automated algorithm for aligning and reslicing PET images. J Comput Assist Tomogr 16:620–633.

Xiong J, Parsons LM, Gao JH, Fox PT (1999): Interregional connectivity to primary motor cortex revealed using MRI resting state images. Hum Brain Mapp 8:151–156.

Yukie M, Iwai E (1985): Laminar origin of direct projection from cortex area V1 to V4 in the rhesus monkey. Brain Res 346:383–386.

Zilles K, Palomero-Gallagher N (2001): Cyto-, myelo-, and receptor architectonics of the human parietal cortex. Neuroimage 14:S8–20.

Zilles K, Schlaug G, Matelli M, Luppino G, Schleicher A, Qu M, Dabringhaus A, Seitz R, Roland PE (1995): Mapping of human and macaque sensorimotor areas by integrating architectonic, transmitter receptor, MRI and PET data. J Anat 187:515–537.